Harriott *et al.*
The Journal of Headache and Pain (2024) 25:152
https://doi.org/10.1186/s10194-024-01855-7

The Journal of Headache and Pain

RESEARCH

Open Access

Oxytocin shortens spreading depolarization-induced periorbital allodynia

Andrea M. Harriott[1*], Melih Kaya[1] and Cenk Ayata[1]

Abstract

Background Migraine is among the most prevalent and burdensome neurological disorders in the United States based on disability-adjusted life years. Cortical spreading depolarization (SD) is the most likely electrophysiological cause of migraine aura and may be linked to trigeminal nociception. We previously demonstrated, using a minimally invasive optogenetic approach of SD induction (opto-SD), that opto-SD triggers acute periorbital mechanical allodynia that is reversed by $5HT_{1B/1D}$ receptor agonists, supporting SD-induced activation of migraine-relevant trigeminal pain pathways in mice. Recent data highlight hypothalamic neural circuits in migraine, and SD may activate hypothalamic neurons. Furthermore, neuroanatomical, electrophysiological, and behavioral data suggest a homeostatic analgesic function of hypothalamic neuropeptide hormone, oxytocin. We, therefore, examined the role of hypothalamic paraventricular nucleus (PVN) and oxytocinergic (OXT) signaling in opto-SD-induced trigeminal pain behavior.

Methods We induced a single opto-SD in adult male and female Thy1-ChR2-YFP transgenic mice and quantified fos immunolabeling in the PVN and supraoptic nucleus (SON) compared with sham controls. Oxytocin expression was also measured in fos-positive neurons in the PVN. Periorbital mechanical allodynia was tested after treatment with selective OXT receptor antagonist L-368,899 (5 to 25 mg/kg i.p.) or vehicle at 1, 2, and 4 h after opto-SD or sham stimulation using von Frey monofilaments.

Results Opto-SD significantly increased the number of fos immunoreactive cells in the PVN and SON as compared to sham stimulation ($p < 0.001$, $p = 0.018$, respectively). A subpopulation of fos-positive neurons also stained positive for oxytocin. Opto-SD evoked periorbital mechanical allodynia 1 h after SD ($p = 0.001$ vs. sham), which recovered quickly within 2 h ($p = 0.638$). OXT receptor antagonist L-368,899 dose-dependently prolonged SD-induced periorbital allodynia ($p < 0.001$). L-368,899 did not affect mechanical thresholds in the absence of opto-SD.

Conclusions These data support an SD-induced activation of PVN neurons and a role for endogenous OXT in alleviating acute SD-induced trigeminal allodynia by shortening its duration.

Keywords Migraine with aura, Spreading depolarization, Oxytocin

Introduction

Migraine is among the top three most burdensome neurological disorders in the United States based on disability adjusted life years [1]. Migraine with aura (MwA) is a subtype of migraine occurring in 20–30% of the migraine population [2]. MwA, while phenotypically heterogeneous, is most commonly characterized by scintillating scotoma followed by severe throbbing headache often with cutaneous allodynia [3–7]. Given the high prevalence

*Correspondence:
Andrea M. Harriott
aharriott@mgb.org
[1] Neurovascular Research Unit, Department of Neurology, Massachusetts General Hospital, 149 13th Street, Charlestown, Boston MA 02129, USA

of migraine, it is projected that there are between 1–1.5 million new cases of MwA every year [1].

Cortical spreading depression (SD) is a wave of neuronal and glial depolarization propagating at a rate of 2-5 mm/min and is the most likely electrophysiological cause of aura [8, 9]. While there have been recent controversies [10, 11], the bulk of preclinical evidence suggests a putative causal link between SD and trigeminal pain. This hypothesis is reinforced by observations that SD increases the firing of trigeminal nociceptors [12]. SD also increases fos expression in medullary dorsal horn [13] and results in increased sensitization of trigeminal brainstem neurons [14]. Moreover, SD induces trigeminal pain behavior [15–17]. Using minimally invasive optogenetic SD induction (opto-SD), we previously showed that opto-SD triggers periorbital mechanical allodynia in mice within 1 h, which was reversed by sumatriptan, a $5HT_{1B/1D}$ receptor agonist and migraine abortive [18]. We also showed more severe allodynia with chronic opto-SD [18]. These data support the view that SD mediates activation of migraine-relevant trigeminal pain pathways in rodents and, by extrapolation, may be able to provoke headache in humans.

Hypothalamic neural circuits are activated before, during, and even after migraine attacks [19, 20] and implicated in migraine initiation and disease phenotype [21]. KCl-induced SD activates neurons in the paraventricular nucleus (PVN) of the hypothalamus [22], which has widespread projections, including to the spinal trigeminal nucleus (Sp5c) [23]. Importantly, emerging data provides evidence that oxytocinergic (OXT) PVN neurons may play an important role in descending pain modulation. For example, OXT can dose-dependently attenuate evoked activity from lamina V wide dynamic range (WDR) neurons receiving Aδ and C fiber inputs from the periorbital region [24, 25] and meninges [26] following peripheral electrical stimulation. This oxytocinergic inhibition of nociceptive activity is blocked by selective oxytocin receptor (OXT-R) antagonist L-368,899 [24–26].

However, the role of hypothalamic PVN neuronal activation and OXT in shaping the amplitude and timing of SD-induced pain behavior remains uncertain. We aimed to identify populations of hypothalamic neurons activated by opto-SD and the role of OXT in modulating opto-SD-induced pain behavioral responses using the selective OXT-R antagonist L-368,899.

Methods

Animals

80 male and female transgenic mice (4–10 months, 22-38 g) expressing channelrhodopsin-2-YFP fusion protein under the thymus cell antigen-1 promoter ($ChR2^+$; B6.Cg-Tg(Thy1-COP4/EYFP)9Gfng/J – Line 9), housed under 12/12-h day/night cycles in temperature-controlled rooms were used for these experiments. Food and water were given ad libitum. All experiments were performed at Massachusetts General Hospital, Charlestown Navy Yard. Experiments received approval from the Institutional Animal Care and Use Committee and were conducted in accordance with the NIH Guide for Care and Use of Laboratory Animals and ARRIVE guidelines.

Spreading depression and drug administration

Procedures for SD induction have been previously described [27]. Briefly, under short duration isoflurane anesthesia, mice underwent scalp incision and placement of a glass coverslip using cyanoacrylate and C&B Metabond one week prior to SD induction. On the day of SD induction, mice were again briefly anesthetized. SD was induced with a 400 μm fiberoptic light source over motor cortex to deliver a 470 nM, 10mW square pulse for 10 s. Single SD was confirmed with intrinsic optical signal difference images using a webcam (OT-HD, Opti-TekScope, Chandler, AZ, USA) interfaced with MATLAB. Mice randomly assigned to sham control groups received coverslip and anesthesia but were not exposed to light stimulation. Following opto-SD, fos staining and mouse behavior were examined in separate cohorts.

Immunohistochemistry (IHC)

1 h after single opto-SD, whole brain was removed and placed in a coronal mouse brain matrix with ventral surface facing up. A block containing the hypothalamus was taken using two blades placed between the optic chiasm rostrally and the ponto-midbrain junction caudally. Brain blocks containing hypothalamus were post-fixed in 4% PFA overnight. Tissue was then submerged in 15% and then 30% sucrose and snap frozen in mounting media using isopentane on dry-ice. For single fos labeling, tissue sections were air dried, washed in 1X phosphate buffered saline (1X PBS) three times for 10 min and incubated in blocking solution (5% normal donkey serum (NDS), 0.5% triton X-100 in 1X PBS) in a humidified chamber for 1 h and then in primary antibody (rabbit anti-c-fos antibody, Abcam, 1:500 in blocking solution) at 4 °C overnight. The following day, tissues were washed three times in 1X PBS (10 min), incubated in secondary antibody (donkey anti-rabbit Alexa fluor 647, Thermofisher 1:500 in 1X PBS) at room temperature for 2 h, washed again and counterstained with DAPI mounting media (Vectashield). For double labeling, tissues were processed as above except they were incubated in blocking solution containing normal goat serum followed by incubation with two primary antibodies (guinea pig anti-c-fos antibody, Synaptic Systems, 1:500; rabbit anti-oxytocin antibody, Abcam, 1:1000 in blocking solution) at 4 °C overnight. The next

day, tissues were incubated with two secondary antibodies (goat anti-guinea pig Alexa fluor 647, Abcam; goat anti-rabbit Alexa Fluor 488, Thermofisher 1:500 in 1X PBS) at room temperature for 2 h prior to wash and DAPI counterstain. Controls included the omission of primary antibody, which did not yield positive nonspecific staining for fos or oxytocin.

Fos-immunoreactivity (fos-IR) was examined in SD and sham animals. The number of fos-positive neurons in the PVN in $n=9$ SD and $n=7$ sham animals and the supraoptic nucleus (SON) in $n=7$ SD and $n=5$ sham animals was quantified. Every fourth brain slice (10 µm thickness) was mounted, a total of 5–6 sections per slide. Every other slide was examined for PVN/SON fos staining. An average of 5.0 ± 0.8 slides per animal in the SD and 5.4 ± 1.2 slides per animal in the sham groups contained PVN. An average of 3.1 ± 0.6 slides per animal in the SD and 3.6 ± 0.7 slides per animal in the sham groups contained SON suggesting even sampling of regions of interest in both groups. Fos positive neurons were identified using Image J software. A sliding paraboloid background subtraction with 50-pixel radius was used to reduce uneven background staining. 'Adjust threshold' function was used to distinguish positive staining from background and 'analyze particle' function to count positively labeled cells with sizes between 150–3000 pixel^2. Image J-generated outline tracings of positive cells were visually inspected for congruence with fos-IR staining (supplemental figure). Cell counts were averaged across slides and presented as mean cell count per slide in the PVN and SON.

Periorbital allodynia

Immediately following opto-SD induction or sham stimulation, intraperitoneal injection of either vehicle or selective oxytocin receptor inhibitor, L-368,899 (Tocris) was administered at doses of 5, 10, or 25 mg/kg. Mechanical periorbital allodynia was examined between the mid-afternoon hours at 1, 2 and 4 h after opto-SD using sequential ascending calibrated von Frey monofilaments (0.008 to 0.4 g, Stoelting Co, Wood Dale, IL, USA), as previously reported, [28, 29] with right and left threshold values averaged.

OXT binds OXTR and vasopressin 1A receptor (V1AR). L-368,899 is a potent, selective small molecule (i.e., nonpeptide) antagonist of the OXTR [30] with a $t_{1/2}$ of 2 h that appears consistent across species when administered intravenously [31]. The C_{max} is reached within 1 h after oral administration of 25 mg/kg in rats. L-368,899 was dissolved in saline to make 0.625 mg/mL solution, aliquoted, and stored at -80°C to be used on the day of the behavior experiment.

Statistical and data analysis, and experimental rigor

Mice were randomized for experiments using an online random number generator (https://www.graphpad.com/quickcalcs/randomize1/). For behavior testing, all experiments were carried out with the investigator blinded to group allocation and unblinded only after the completion of data collection. For sample size determination, using existing variability of prior data (σ 0.014 – 0.12), a sample size of $n=8$ per group was estimated assuming power ≥ 80%, $\alpha=0.05$ for periorbital allodynia testing. Males and females were balanced per group. Statistical analyses for each dataset are indicated in the results section and figure legends. All statistical analyses are conducted using GraphPad Prism 7.0. For all testing, two-tailed $p<0.05$ was considered statistically significant. Parametric data analysis was performed unless data were not normally distributed (e.g., periorbital allodynia), in which case data were rank transformed. Data are presented as mean ± standard error (SEM) or median ± 25th,75th percentile.

Results

SD induces c-fos expression in oxytocinergic PVN neurons of the hypothalamus

On visual inspection, SD-induced fos immunoreactivity (fos-IR) was found in the ipsilateral cerebral cortex, piriform cortex, and thalamus (supplemental figure). There was dense fos-IR in the bilateral paraventricular nucleus (PVN) of the hypothalamus following SD, as previously described [22]. Oxytocin (OXT) is expressed in the PVN, SON and intermediate accessory nuclei of the hypothalamus with widespread projections [32, 33]. Furthermore, OXT PVN neurons send projections to OXT expressing SON neurons to form anatomical and functional connections that may be important for modulating pain [33, 34]. SD produced robust fos-IR in both the PVN and SON. While PVN and SON share expression of other neuropeptides, activation of neurons in both regions would be consistent with activation of an OXT neural circuit. Based on the pattern of fos staining and the putative role of OXT in pain modulation, quantification of fos staining and colocalization with OXT were examined in PVN and SON.

Single opto-SD increased the number of fos-IR cells in the PVN compared to sham (122.4 ± 11.1 vs. 24.9 ± 7.2, respectively, $p<0.001$, t-test). Likewise, there was robust SD-induced increases in fos-IR in the SON compared to sham (43.5 ± 4.1 vs. 25.7 ± 4.7, respectively, $p=0.018$, t-test). OXT is expressed in magnocellular and parvocellular neurons of the PVN and SON with broad projections to limbic (amygdala, bed nucleus of the stria terminalis) and brainstem (medullary dorsal horn,

periaqueductal grey) areas [24–26, 33, 35, 36]. A subpopulation of SD-induced fos-positive PVN neurons were also positive for OXT (11.54 ± 2.03% fos-IR neurons stain positive for OXT and 14.62 ± 1.72% OXT-IR neurons stain positive for fos in SD mice, Fig. 1).

Oxytocin mediates recovery from SD-induced periorbital allodynia

To examine the putative role of OXT neuron activation in SD-induced trigeminal pain, animals were divided into four groups ($n = 8$/group), each receiving a single opto-SD or sham stimulation and OXTR antagonist L-368,899 (5, 10, or 25 mg/kg i.p.) or vehicle (i.e., two-by-two design) immediately after SD. Periorbital allodynia was tested at 1, 2 and 4 h after opto-SD.

After sham stimulation, L-368,899 (5, 10, or 25 mg/kg i.p.) did not significantly alter periorbital mechanical thresholds compared with vehicle at any time point (Fig. 2). Opto-SD significantly reduced periorbital threshold compared to sham 1 h after stimulation in all treatment arms ($p < 0.001$, $p = 0.003$, $p < 0.001$, $p < 0.001$ at 0 (i.e., vehicle), 5, 10 and 25 mg/kg L-368,899, respectively) [18, 27, 37]. In vehicle-treated mice, opto-SD-induced acute periorbital allodynia completely resolved within 2 h ($p = 0.638$ and $p = 0.990$ at 2 and 4 h, respectively). L-368,899 dose-dependently delayed the recovery of periorbital allodynia. While 5 mg/kg was ineffective ($p = 0.923$ and 0.911 at 2 and 4 h, respectively), 10 mg/kg prevented the recovery at 2 h ($p = 0.005$) but not at 4 h ($p = 0.409$). At 25 mg/kg dose level, opto-SD-induced periorbital allodynia persisted at 4 h ($p < 0.001$ at 2 and 4 h). The relative EC50 at 4 h was 16 mg/kg.

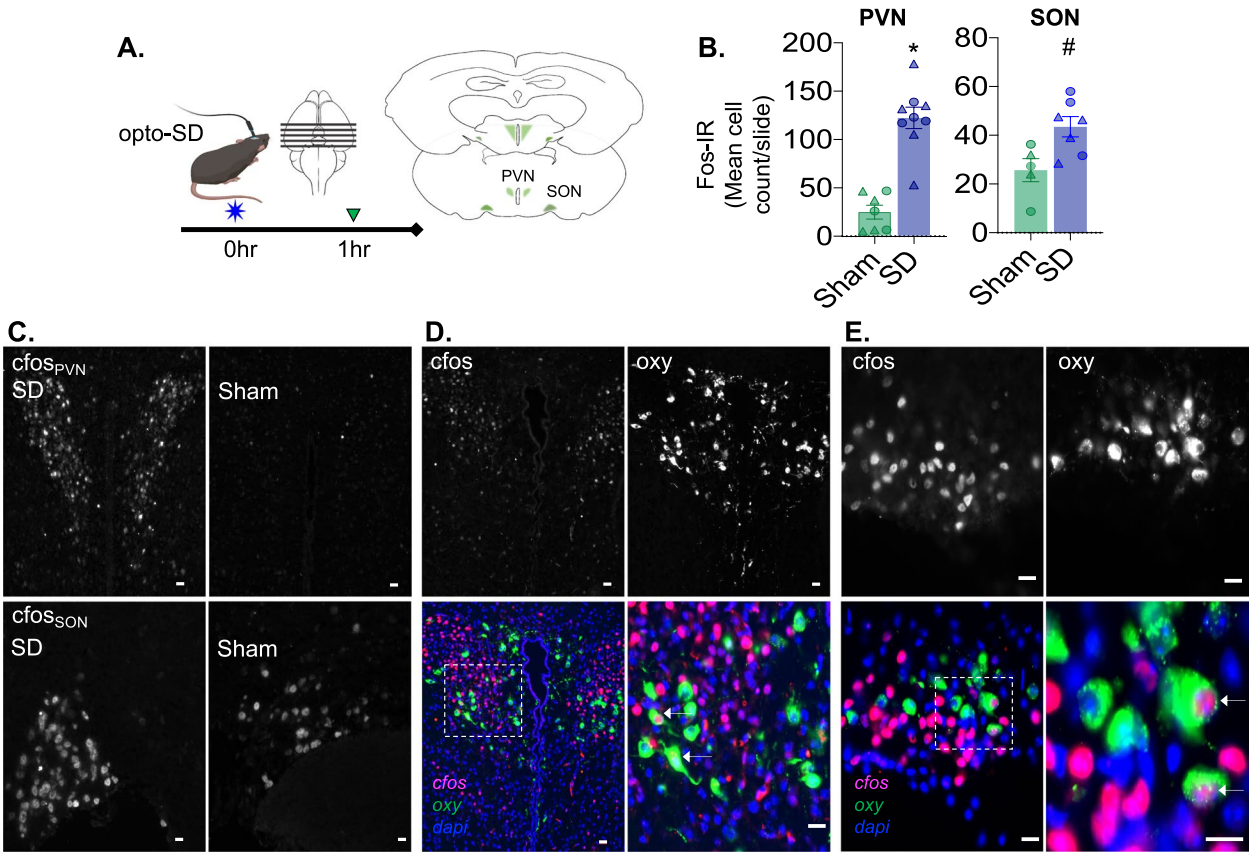

Fig. 1 Opto-SD increases fos-IR in PVN and SON and co-localizes with oxytocin. **A** Single opto-SD was induced 1 h prior to removal of a tissue block containing the hypothalamus. 10 µM thick tissue sections were stained for fos. **B** SD ($n = 9$), significantly increased the number of fos postive cells in the PVN as compared to sham ($n = 7$). In tissue sections where SON was identified, SD ($n = 7$) also produced a significant increase in the number of fos positive cells as compared to sham ($n = 5$). Males are represented as circles and females as triangles. Because of the sample size, sex differences were not tested. *$p < 0.0001$, #$p = 0.0182$, unpaired t-test. **C** Left upper panel shows symmetric fos staining in the PVN following SD, and right upper panel following sham stimulation. Fos-IR in SON following SD and sham stimulation are shown in the left lower and right lower panels respectively. **D** In the right upper panels fos and oxytocin staining are shown following SD. The lower panel shows colocalization of fos and oxytocin in some PVN cells in an example of a merged image (arrows are shown in the magnified image to the right). **E** Demonstrates the same for SON following SD. Bar = 100 µM

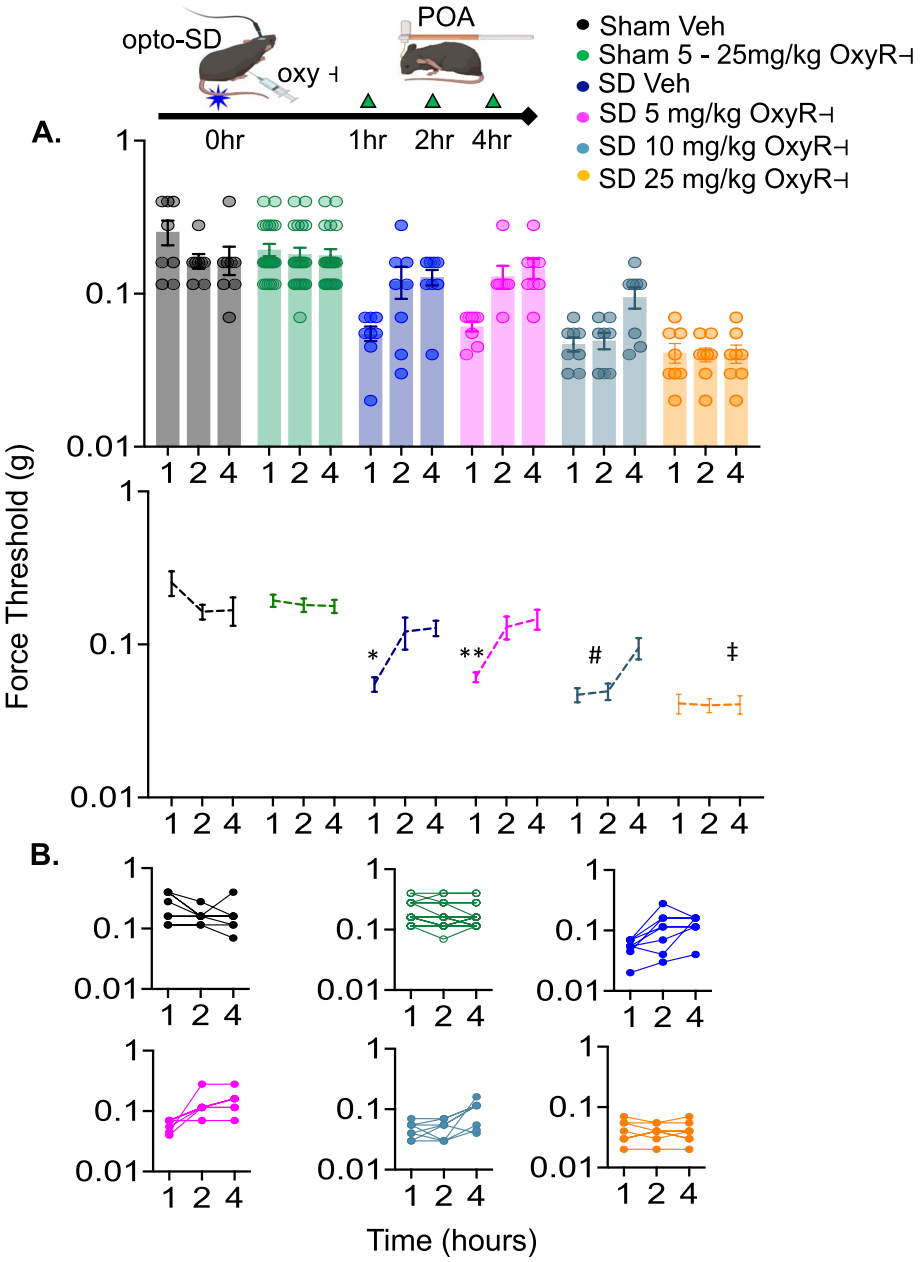

Fig. 2 Oxytocin receptor antagonist (L-368,899, Oxy-R ⊣) prolongs opto-SD-induced acute periorbital allodynia ($n = 8$/group). **A** Following opto-SD, vehicle or oxytocin receptor antagonist (5, 10 and 25 mg/kg in 3 separate groups) was administered via intraperitoneal injection. Periorbital mechanical allodynia was tested 1, 2 and 4 h later. There was no significant effect of Oxy-R antagonist on periorbital thresholds in sham mice at any dose tested. Opto-SD produced periorbital allodynia at 1 h which recovered by 2 h. At low doses of Oxy-R antagonist (5 mg/kg), there was no effect on opto-SD induced periorbital allodynia. However, with increasing doses, mice displayed longer lasting periorbital allodynia. In the presence of Oxy-R antagonist 10 mg/kg, opto-SD produced periorbital allodynia that lasted 2 h and in the presence of Oxy-R antagonist 25 mg/kg, opto-SD produced periorbital allodynia that lasted at least 4 h. **B** Shows individual data for each animal tested for each dose of vehicle or drug per group. * $p = 0.001$, ** $p = 0.003$, # $p = 0.0003$ at 1 h, $p = 0.005$ at 2 h, ‡ $p < 0.0001$ at 1, 2 and 4 h; two-way ANOVA, Tukey's post-hoc analysis

While sex differences were not the primary end point of this study, multivariable regression revealed a significant three-way interaction among the variables sex, opto-SD (vs. sham) and L-368,899 dose (0–25 mg/kg) on lowering periorbital threshold ($p < 0.001$) such that females appeared more sensitive to higher doses of the drug. There were also significant interactions between SD and recovery over time from allodynia across sex as previously demonstrated [37] (Table 1).

Table 1 Multiple regression analysis of SD-induced Periorbital Allodynia

Variable	Estimate	95% CI		Std error	|t|	p-value	F (DFn, DFd)
SD vs Sham	-67.25	-82.01	-52.48	7.48	8.99	< 0.0001	F (1, 182) = 80.75
Drug dose	0.14	-0.64	0.93	0.40	0.36	0.718	F (1, 182) = 0.13
Time	5.22	0.15	10.28	2.57	2.03	0.044	F (1, 182) = 4.13
Sex	2.92	-12.23	18.06	7.67	0.38	0.704	F (1, 182) = 0.14
Age	0.76	-2.30	3.82	1.55	0.49	0.626	F (1, 182) = 0.24
SD vs Sham: Dose: Time	-0.39	-0.76	-0.02	0.19	2.08	0.039	F (1, 182) = 4.32
SD vs Sham: Dose: Sex	-2.32	-3.62	-1.02	0.66	3.51	0.001	F (1, 182) = 12.31
SD vs Sham: Time: Sex	12.24	4.97	19.52	3.69	3.32	0.001	F (1, 182) = 11.02

A multivariable regression was performed examining the effect of SD on periorbital threshold controlling for sex, age, time between SD and allodynia testing, and dose of OXTR antagonist L-368,899. The overall model was significant ($F = 28.48$, $p < 0.0001$). There was no effect of age on periorbital threshold. SD was significantly associated with lower thresholds. Time was significantly associated with recovery from periorbital allodynia. There were significant three-way interactions demonstrating the effect of SD and drug dose on periorbital threshold varies across time such that higher drug doses reduced recovery from allodynia. Additionally, three-way interactions with sex demonstrated SD and recovery from allodynia as well as SD and drug dose varied across sex

Discussion

Our data suggest opto-SD can activate neurons in the PVN, some of which are oxytocinergic. Following single minimally invasive opto-SD, there was robust fos-staining in the bilateral PVN and colocalization of fos with oxytocin immunoreactivity in some but not all fos-IR neurons. Our data also demonstrated that while selective OXTR antagonist did not affect baseline trigeminal pain, it dose-dependently prolonged opto-SD-induced periorbital allodynia. These data support the hypothesis that SD activates oxytocinergic neural circuits and further suggests that the role of oxytocin may be to alleviate SD-induced trigeminal pain by shortening the duration of periorbital allodynia.

SD and activation of PVN neurons

Our study findings are consistent with prior observations that SD activates hypothalamic neural circuits. In one study, 1 M cotton ball soaked KCl applied to the dural surface produced recurrent SD and increased fos-immunolabeling in magnocellular PVN neurons compared to aCSF application [22]. Furthermore, there is existing indirect evidence that SD may activate hypothalamic oxytocinergic neural circuits. SD triggered by electrophoretic application of K^+ using 1 mA current stimulus over silver wire in glass electrodes filled with 25% KCl or pressure injection of 6% KCl elicits bouts of yawning behavior in male hooded rats [38]. While other neurohormones and neurotransmitters are involved in this behavior, dopaminergic activation of oxytocinergic neurons facilitates yawning [39]. Our observation that opto-SD produces fos expression in oxytocinergic PVN neurons is consistent with an SD-mediated increase in yawning. Indeed, migraine with aura has also been associated with repetitive yawning during the headache phase [40]. Other forms of cortical excitation also activate oxytocinergic PVN neurons, though the patterns of activation differ. For example, kainic acid evoked seizures elicits fos expression in oxytocinergic PVN neurons [41]. These data suggest strong depolarizing cortical stimulation may induce stress adaptive responses capable of activating PVN neural circuits [41].

SD in rodent lissencephalic cortex is holohemispheric, raising the possibility that a more restricted pattern of SD propagation observed in gyrencephalic cortex may not produce a stimulus sufficiently robust to activate PVN neurons to the extent observed in this study. Equally, it is possible that direct propagation of SD into prefrontal cortex is needed to produce hypothalamic neuronal activation [42] and that such widespread SD propagation would rarely occur in gyrencephalic brain [43, 44]. However, while most afferent inputs to the PVN and SON are bilateral, cortical afferent projections are ipsilateral from prelimbic, agranular insular, cingulate and amygdaloid cortex [45, 46]. Importantly, we found increases in PVN fos expression ipsilateral and contralateral to single cortical opto-SD induction. Based on these neuroanatomical connections, it is unlikely that opto-SD-induced bilateral PVN fos expression is explained by propagation into prefrontal cortex. Rather activation of other neural circuits including ascending trigeminohypothalamic [47, 48], and/or thalamic inputs [45] may explain this bilateral pattern of fos activation.

Anti-nociceptive effects of OXT

We focused on OXT because of its emerging role in trigeminal analgesia [24–26, 49]. PVN electrical stimulation inhibits meningeal WDR neurons in Sp5c. This inhibitory effect was blocked by OXTR antagonist [25, 26]. Indeed, exogenous OXT dose-dependently inhibits Aδ and C fiber nociceptive input to Sp5c WDR lamina V neurons with cutaneous supraorbital receptive fields.

Treatment with L-368,899 prevented OXT inhibition of Sp5c neuronal activity. However selective V1AR inhibitor, SR-49059 did not [24]. These data suggest OXT may play an important role in the pathology of cranial pain disorders via descending inhibition of nociceptive input. Further, these data identify OXT and OXTR as a viable antimigraine therapeutic target.

To date for migraine, this has only been supported by a behavioral study using a nitroglycerin (NTG) migraine mouse model and preliminary clinical studies. In a model of chronic migraine without aura in which NTG was administered every other day for 11 days, repeated exogenous administration of intranasal OXT produced robust inhibition of NTG-induced hindpaw and periorbital mechanical allodynia [50]. There was an NTG-mediated increase in OXTR expression in the trigeminal nucleus caudalis (TNC). Moreover, NTG increased fos staining and phosphorylated N-methyl D-aspartate receptor subunit (NR2B) expression in the TNC. These changes were reversed by OXT administration [50]. Importantly, our data demonstrate that OXT is likely involved in intrinsic homeostatic responses important for mitigating opto-SD or events downstream of opto-SD as OXT was not administered exogenously but OXTR antagonist was able to prolong the effect of opto-SD on pain behavior. Taken together, these data indeed provide compelling preclinical evidence for a potential anti-migraine therapeutic benefit of OXT.

Data from OXT pilot studies have been published in a review that describes results of a double-blind pilot trial testing a single dose of intranasal OXT which demonstrated a non-significant trend in greater subject satisfaction at 24 h compared to placebo for acute treatment of episodic migraine though there was no effect on the proportion of patients experiencing significant 2-h headache relief [51]. In a chronic migraine population, intranasal OXT for acute treatment of migraine attacks alleviated headache in a greater proportion of patients at 4 h, but not 2 h compared to placebo. There were additional open label pilot studies of OXT for migraine prevention suggesting a reduction in migraine attack frequency [51]. Certainly, larger clinical studies including dose finding studies might be informative to understand the clinical efficacy of OXT.

OXT as a putative anti-migraine therapeutic target

The anti-nociceptive effect of OXT is not selective for trigeminal pain. There is evidence that OXT also plays a role in spinal analgesia [34, 52–54]. Activation of PVN neurons can alleviate CFA-mediated hindpaw mechanical allodynia and heat hyperalgesia [34]. 1.5% carrageenan injection into the hindpaw produces paw withdrawal whose latency is increased with intrathecal OXT administration. However, the dose needed to produce an analgesic effect in female mice was an order of magnitude higher (1.25 nmol OXT) as compared to males (0.125 nmol OXT) suggesting sex differences in oxytocinergic mechanisms of pain modulation [55]. Similar results were obtained with formalin hindpaw injection [56]. Most data with spinal nerve injury models also provide evidence that OXT plays a role in spinal analgesia. While chemogenetic inhibition of PVN oxytocinergic neurons exacerbated pain responses in CFA treated rats, it did not have an effect in cuff pressure sciatic nerve injury animals suggesting OXT modulates pain in most but not all spinal pain states [34]. In contrast, intrathecal OXT reduced loose ligature sciatic nerve injury-induced cold allodynia in response to topical acetone and mechanical allodynia [53]. Analgesic effects have also been demonstrated in partial sciatic nerve injury model [56].

Taken together, these data support an inhibitory role of PVN OXT neurons in most spinal inflammatory and nerve injury models with potential sex differences in response and suggest a general role of OXT in limiting the experience of pain across a wide variety of pain states.

Site of action of oxytocin

The major site of neuronal OXT expression is in the PVN and SON. OXT is released into the systemic circulation via the neurohypophysis and also acts as a neurotransmitter via widespread oxytocinergic projections [57]. While the proposed site of analgesic action of OXT is at the level of the TNC given the expression of OXTR on medullary dorsal horn neurons and descending projection of PVN neurons to this region [58], other regions receiving oxytocinergic projections from the PVN may also be involved in shaping pain behavior. For example, PVN OXT neurons project to the rostral angular insular cortex where OXT microinjection dose-dependently reduces formalin-induced flinching behavior, likely via GABAergic and noradrenergic descending pain modulation [59]. Additionally, there are direct PVN to prelimbic prefrontal cortex (PFC) projections and OXT injection into PFC inhibits chronic inflammatory pain behavior in a CFA hindpaw model [60]. Moreover, OXTR is also expressed on CGRP containing trigeminal neurons, raising the possibility that additional anti-nociceptive effects may be mediated via inhibitory action on peripheral nociceptors [61].

Selective OXTR antagonist L-368,899 in this study enhanced the acute SD-induced pain behavior in a dose-dependent manner (10 and 25 mg/kg i.p.). While lower doses of antagonist were used in studies examining appetitive and taste aversion behavior in mice (1-3 mg/kg i.p.) [62], higher doses (5-10 mg/kg i.p.) have been used to

examine hyperaggressive behavior, social interaction and fear avoidance behavior [63–65]. Also, based on the pharmacokinetic profile of the OXTR antagonist in rat and dog at 10 mg/kg i.v. and 100 mg/kg oral dosing (plasma $t_{1/2}$ ~ 2 h and 2–4 h respectively)[31], we expect the drug to be biologically active at the timepoints tested. However, since L-368,899 can readily cross the BBB [66], it is not able to distinguish between central and peripheral actions of OXT. It is therefore plausible that SD-induced activation of PVN OXT neurons could target peripheral, central, medullary, limbic and/or supralimbic OXTR to shape pain behavior and each of these neural circuits could be playing a relevant role in shaping pain behavior and therefore could be potential targets of future drug therapies.

Duration and characteristics of SD-induced allodynia

Several studies demonstrate acute allodynia following SD. However, the duration of allodynia varies from 1–5 h. The difference in duration may be attributed to differences in assessment of behavior, procedures used to induce SD (i.e. craniotomy), SD induction methods (i.e. KCl, pinprick trauma or optogenetic techniques), and SD number (single vs. repetitive SD). Additionally, there is intrinsic variability in neuronal response to SD. For example, while the timing of SD-induced activation of cervicomedullary neurons may not correlate with the exact timing of behavior, pinprick trauma and KCl-induced SD increase baseline firing in nearly 50% of neurons with differences in duration of activation. For some neurons activation lasts 30 min while in others activation lasts nearly 2 h (throughout the recording period). The variability in onset, duration and rate of increase in firing is attributed to SD induction methods [14]. The pattern and duration of SD-induced activation of meningeal nociceptors likewise vary [12]. In a behavioral study examining opto-SD, the reduction in periorbital force threshold lasted for at least 3 h [67]. While both this study and our study used opto-SD, the method of stimulation differed. To induce SD in occipital cortex, this study produced a burrhole and cortical injection of adeno-associated viral vector containing Chr2 [67] which may have contributed to the longer lasting allodynia response. Lastly, it should be noted that periorbital allodynia is a surrogate measure of activation of trigeminal nociceptive pathways. Its validity for use in preclinical migraine studies is based on the observation that patients experience cutaneous allodynia [7] likely mediated by central sensitization. Like previous observations [18], unilateral SD produced bilateral periorbital allodynia. Indeed, unilateral SD produces bilateral activation of subcortical and brainstem areas involved in pain processing [22, 68]. Spread of allodynia to bilateral regions has also been described in clinical studies [69] and may be attributed to recruitment of supramedullary nociceptive neurons [70].

Study limitations

There are several study limitations. We did not directly record from PVN neurons following opto-SD but rather used fos expression as a marker of neuronal activation. While fos expression has been reliably used as a marker of neural activity for decades, its expression may be incomplete [71, 72]. Therefore, SD-induced timing and pattern of changes in PVN neuronal firing are still unexplored areas of investigation. Opto-SD-induced fos positive neurons in the PVN stained positive and negative for OXT with colocalization between fos and OXT representing 12% of the fos population and 15% of the OXT population. The PVN contains a diverse population of descending projection neurons, including dynorphinergic, enkephalinergic and vasopressinergic neurons [73, 74]. The role of these neuronal subpopulations in migraine-relevant pain behavior and other cardiovascular and cerebrovascular phenotypes associated with aura remains unclear. Indeed, other methods including spatial transcriptomics may be useful in identifying other subpopulations of the PVN activated by SD. Additionally, in our study, higher doses of drug in females appeared to exacerbate opto-SD-induce periorbital allodynia as compared to males with a significant three-way interaction between sex, opto-SD, and drug. This effect is likely related to sex-differences in pharmacokinetics of L-368,899. At higher i.v. doses, clearance of drug in females is reduced. Additionally, the plasma concentration area under the curve is higher in females suggesting sex differences in drug metabolism and pharmacodynamics which may affect studies using this antagonist when examining higher doses of drug [31]. Lastly, mechanisms of SD and SD morphology may differ depending on method of induction [75, 76], species selection [77], or sleep/wake states [78]. Similarly, the degree and pattern of SD spread differ in gyriform cortex [43, 44]. Resultingly, it is possible that trigeminal pain phenotypes are amplified in mouse SD models and that the pattern of trigeminal responses, their duration, and activation of other neural circuits including hypothalamic neural circuits may differ in anesthetized lissencephalic cortical SD. While the behavioral experiments in non-primate mammals with gyrencephalic cortex may be possible, there are limitations in their feasibility. However, emerging tools are becoming more widely available to study differences in awake SD and subsequent pain phenotypes [79]. However, as both sham and SD mice were exposed to anesthesia, we believe the SD-induced activation of PVN neurons is mediated by the effect of SD. Moreover, similar patterns of PVN neuronal activation have been observed in other models of somatic and trigeminal pain [80, 81] suggesting a broader role of the PVN in pain modulation.

Conclusions

Despite limitations, to date, neuroanatomical, electrophysiological, and behavioral data suggest a homeostatic analgesic function of OXT [82]. Data presented here support an SD-induced activation of PVN neurons and a role for endogenous OXT in alleviating acute SD-induced trigeminal allodynia by shortening its duration.

Supplementary Information

The online version contains supplementary material available at https://doi.org/10.1186/s10194-024-01855-7.

Supplementary Material 1: Supplemental figure. Fos staining and cell count using Image J. A. Fos staining was seen following SD in ipsilateral cerebral cortex, piriform cortex, bilateral thalamus and bilateral PVN. B. and C. demonstrate fos staining for ipsilateral vs contralateral cortex following SD and D. and E. from ipsilateral vs contralateral piriform cortex respectively. F. demonstrates fos staining in the PVN of the thalamus. In G. and H., hypothalamic PVN sections with fos staining demonstrating differences in intensity of fos-IR after background subtraction. H. demonstrates particle identification above background with arrow showing cells that are juxtapositioned split with a binary watershed processing feature

Acknowledgements
The authors would like to thank Andreia Morais, PhD for her his kind assistance and technical support during this project.

Authors' contributions
(AH) research design, data acquisition, data analysis, data interpretation, reagents or supplies, drafted or revised manuscript; (MK) data acquisition, data analysis; (CA) research design, revised manuscript. All authors reviewed the manuscript.

Funding
AH K08NS124991.

Availability of data and materials
Data are freely available from the corresponding author upon request.

Data availability
No datasets were generated or analysed during the current study.

Declarations

Competing interests
AH is on the Board of Directors of the American Headache Society, American Migraine Foundation and Headache Cooperative of New England, has served on Scientific Advisory Board for Theranica and Abbvie.

Received: 7 July 2024 Accepted: 2 September 2024
Published online: 17 September 2024

References

1. Collaborators GUND et al (2021) Burden of Neurological Disorders Across the US From 1990–2017: A Global Burden of Disease Study. JAMA Neurol 78(2):165–176
2. Rasmussen B.K., Olesen J (1992) Migraine with aura and migraine without aura: an epidemiological study. Cephalalgia. 12(4):221–8 (discussion 186)
3. Viana M et al (2019) Clinical features of visual migraine aura: a systematic review. J Headache Pain 20(1):64
4. Viana M et al (2017) Clinical features of migraine aura: Results from a prospective diary-aided study. Cephalalgia 37(10):979–989
5. Hansen JM, Goadsby PJ, Charles AC (2016) Variability of clinical features in attacks of migraine with aura. Cephalalgia 36(3):216–224
6. Russell MB, Olesen J (1996) A nosographic analysis of the migraine aura in a general population. Brain 119(Pt 2):355–361
7. Lipton RB et al (2008) Cutaneous allodynia in the migraine population. Ann Neurol 63(2):148–158
8. Ayata C (2010) Cortical spreading depression triggers migraine attack: pro. Headache 50(4):725–730
9. Hadjikhani N et al (2001) Mechanisms of migraine aura revealed by functional MRI in human visual cortex. Proc Natl Acad Sci U S A 98(8):4687–4692
10. Mehnert J, Fischer-Schulte L, May A (2023) Aura phenomena do not initiate migraine attacks-Findings from neuroimaging. Headache 63(8):1040–1044
11. Goadsby PJ (2001) Migraine, aura, and cortical spreading depression: why are we still talking about it? Ann Neurol 49(1):4–6
12. Zhang X et al (2010) Activation of meningeal nociceptors by cortical spreading depression: implications for migraine with aura. J Neurosci 30(26):8807–8814
13. Moskowitz MA, Nozaki K, Kraig RP (1993) Neocortical spreading depression provokes the expression of c-fos protein-like immunoreactivity within trigeminal nucleus caudalis via trigeminovascular mechanisms. J Neurosci 13(3):1167–1177
14. Zhang X et al (2011) Activation of central trigeminovascular neurons by cortical spreading depression. Ann Neurol 69(5):855–865
15. Filiz A et al (2019) CGRP receptor antagonist MK-8825 attenuates cortical spreading depression induced pain behavior. Cephalalgia 39(3):354–365
16. Cottier, K.E., et al., Loss of Blood-Brain Barrier Integrity in a KCl-Induced Model of Episodic Headache Enhances CNS Drug Delivery. eNeuro, 2018. **5**(4).
17. Tang C et al (2020) Cortical spreading depolarisation-induced facial hyperalgesia, photophobia and hypomotility are ameliorated by sumatriptan and olcegepant. Sci Rep 10(1):11408
18. Harriott AM et al (2021) Optogenetic Spreading Depression Elicits Trigeminal Pain and Anxiety Behavior. Ann Neurol 89(1):99–110
19. Denuelle M et al (2007) Hypothalamic activation in spontaneous migraine attacks. Headache 47(10):1418–1426
20. Schulte LH, May A (2016) The migraine generator revisited: continuous scanning of the migraine cycle over 30 days and three spontaneous attacks. Brain 139(Pt 7):1987–1993
21. Burstein R, Jakubowski M (2005) Unitary hypothesis for multiple triggers of the pain and strain of migraine. J Comp Neurol 493(1):9–14
22. Iqbal Chowdhury GM et al (2003) Cortical spreading depression affects Fos expression in the hypothalamic paraventricular nucleus and the cerebral cortex of both hemispheres. Neurosci Res 45(2):149–155
23. Abdallah, K., et al., Correction: Bilateral Descending Hypothalamic Projections to the Spinal Trigeminal Nucleus Caudalis in Rats. PLoS One, 2013. **8**(9).
24. Garcia-Boll E et al (2018) Oxytocin inhibits the rat medullary dorsal horn Sp5c/C1 nociceptive transmission through OT but not V(1A) receptors. Neuropharmacology 129:109–117
25. Condes-Lara, M., et al., Hypothalamic Paraventricular Stimulation Inhibits Nociceptive Wide Dynamic Range Trigeminocervical Complex Cells via Oxytocinergic Transmission. J Neurosci, 2024. **44**(17).
26. Garcia-Boll E et al (2020) Inhibition of nociceptive dural input to the trigeminocervical complex through oxytocinergic transmission. Exp Neurol 323:113079
27. Morais A et al (2023) Inhibition of persistent sodium current reduces spreading depression-evoked allodynia in a mouse model of migraine with aura. Pain 164(11):2564–2571
28. Elliott MB et al (2012) Nociceptive neuropeptide increases and periorbital allodynia in a model of traumatic brain injury. Headache 52(6):966–984
29. Deuis JR, Dvorakova LS, Vetter I (2017) Methods Used to Evaluate Pain Behaviors in Rodents. Front Mol Neurosci 10:284
30. P.D Williams et al (1994) 1-((7,7-Dimethyl-2(S)-(2(S)-amino-4-(methylsulfonyl) butyramido)bicyclo [2.2.1]-heptan-1(S)-yl)methyl)sulfonyl)-4-(2-methylphenyl)piperaz ine (L-368,899): an orally bioavailable, non-peptide oxytocin antagonist with potential utility for managing preterm labor. J Med Chem. 37(5):565–71

31. Thompson KL et al (1997) Pharmacokinetics and disposition of the oxytocin receptor antagonist L-368,899 in rats and dogs. Drug Metab Dispos 25(10):1113–1118
32. Maejima Y et al (2018) The Anorexigenic Neural Pathways of Oxytocin and Their Clinical Implication. Neuroendocrinology 107(1):91–104
33. Liao PY et al (2020) Mapping Central Projection of Oxytocin Neurons in Unmated Mice Using Cre and Alkaline Phosphatase Reporter. Front Neuroanat 14:559402
34. Eliava M et al (2016) A New Population of Parvocellular Oxytocin Neurons Controlling Magnocellular Neuron Activity and Inflammatory Pain Processing. Neuron 89(6):1291–1304
35. Son S et al (2022) Whole-Brain Wiring Diagram of Oxytocin System in Adult Mice. J Neurosci 42(25):5021–5033
36. Froemke RC, Young LJ (2021) Oxytocin, Neural Plasticity, and Social Behavior. Annu Rev Neurosci 44:359–381
37. Harriott AM et al (2023) The effect of sex and estrus cycle stage on optogenetic spreading depression induced migraine-like pain phenotypes. J Headache Pain 24(1):85
38. Huston J (1971) Yawning and penile erection induced in rats by cortical spreading depression. Nature 232(5308):274–275
39. Argiolas A, Melis MR (1998) The neuropharmacology of yawning. Eur J Pharmacol 343(1):1–16
40. Guven B, Guven H, Comoglu SS (2018) Migraine and Yawning. Headache 58(2):210–216
41. Piekut DT, Pretel S, Applegate CD (1996) Activation of oxytocin-containing neurons of the paraventricular nucleus (PVN) following generalized seizures. Synapse 23(4):312–320
42. Shibata M et al (1984) Activity of hypothalamic thermosensitive neurons during cortical spreading depression in the rat. Brain Res 308(2):255–262
43. Santos E et al (2017) Heterogeneous propagation of spreading depolarizations in the lissencephalic and gyrencephalic brain. J Cereb Blood Flow Metab 37(7):2639–2643
44. Santos E et al (2014) Radial, spiral and reverberating waves of spreading depolarization occur in the gyrencephalic brain. Neuroimage 99:244–255
45. Wei HH et al (2021) Presynaptic inputs to vasopressin neurons in the hypothalamic supraoptic nucleus and paraventricular nucleus in mice. Exp Neurol 343:113784
46. Silverman AJ, Oldfield BJ (1984) Synaptic input to vasopressin neurons of the paraventricular nucleus (PVN). Peptides 5(Suppl 1):139–150
47. Malick A, Burstein R (1998) Cells of origin of the trigeminohypothalamic tract in the rat. J Comp Neurol 400(1):125–144
48. Malick A, Strassman RM, Burstein R (2000) Trigeminohypothalamic and reticulohypothalamic tract neurons in the upper cervical spinal cord and caudal medulla of the rat. J Neurophysiol 84(4):2078–2112
49. Warfvinge K et al (2020) Oxytocin as a regulatory neuropeptide in the trigeminovascular system: Localization, expression and function of oxytocin and oxytocin receptors. Cephalalgia 40(12):1283–1295
50. Wang Y et al (2021) Repeated oxytocin prevents central sensitization by regulating synaptic plasticity via oxytocin receptor in a chronic migraine mouse model. J Headache Pain 22(1):84
51. Tzabazis A et al (2017) Oxytocin and Migraine Headache. Headache 57(Suppl 2):64–75
52. Condes-Lara M et al (2009) Hypothalamospinal oxytocinergic antinociception is mediated by GABAergic and opiate neurons that reduce A-delta and C fiber primary afferent excitation of spinal cord cells. Brain Res 1247:38–49
53. Condes-Lara M et al (2006) Paraventricular hypothalamic influences on spinal nociceptive processing. Brain Res 1081(1):126–137
54. Rojas-Piloni G et al (2008) Nociceptive spinothalamic tract and postsynaptic dorsal column neurons are modulated by paraventricular hypothalamic activation. Eur J Neurosci 28(3):546–558
55. Chow LH et al (2016) Sex Difference in Oxytocin-Induced Anti-Hyperalgesia at the Spinal Level in Rats with Intraplantar Carrageenan-Induced Inflammation. PLoS ONE 11(9):e0162218
56. Nishimura H et al (2022) Endogenous oxytocin exerts anti-nociceptive and anti-inflammatory effects in rats. Commun Biol 5(1):907
57. Gimpl G, Fahrenholz F (2001) The oxytocin receptor system: structure, function, and regulation. Physiol Rev 81(2):629–683
58. Abdallah K et al (2013) Bilateral descending hypothalamic projections to the spinal trigeminal nucleus caudalis in rats. PLoS ONE 8(8):e73022
59. Gamal-Eltrabily M et al (2020) The Rostral Agranular Insular Cortex, a New Site of Oxytocin to Induce Antinociception. J Neurosci 40(29):5669–5680
60. Liu Y et al (2023) Oxytocin promotes prefrontal population activity via the PVN-PFC pathway to regulate pain. Neuron 111(11):1795-1811 e7
61. Tzabazis A et al (2016) Oxytocin receptor: Expression in the trigeminal nociceptive system and potential role in the treatment of headache disorders. Cephalalgia 36(10):943–950
62. Olszewski PK et al (2013) Oxytocin receptor blockade reduces acquisition but not retrieval of taste aversion and blunts responsiveness of amygdala neurons to an aversive stimulus. Peptides 50:36–41
63. Tan O et al (2019) Oxytocin and vasopressin inhibit hyper-aggressive behaviour in socially isolated mice. Neuropharmacology 156:107573
64. Harshaw C et al (2021) Oxytocin and "social hyperthermia": Interaction with beta(3)-adrenergic receptor-mediated thermogenesis and significance for the expression of social behavior in male and female mice. Horm Behav 131:104981
65. Pisansky MT et al (2017) Oxytocin enhances observational fear in mice. Nat Commun 8(1):2102
66. Boccia ML et al (2007) Peripherally administered non-peptide oxytocin antagonist, L368,899, accumulates in limbic brain areas: a new pharmacological tool for the study of social motivation in non-human primates. Horm Behav 52(3):344–351
67. Pi C et al (2022) Cortical pain induced by optogenetic cortical spreading depression: from whole brain activity mapping. Mol Brain 15(1):99
68. Borysovych Bogdanov V et al (2015) Cortical spreading depression decreases Fos expression in rat periaqueductal gray matter. Neurosci Lett 585:138–143
69. Cooke L, Eliasziw M, Becker WJ (2007) Cutaneous allodynia in transformed migraine patients. Headache 47(4):531–539
70. Burstein R, Cutrer MF, Yarnitsky D (2000) The development of cutaneous allodynia during a migraine attack clinical evidence for the sequential recruitment of spinal and supraspinal nociceptive neurons in migraine. Brain 123(Pt 8):1703–1709
71. Bullitt E (1990) Expression of c-fos-like protein as a marker for neuronal activity following noxious stimulation in the rat. J Comp Neurol 296(4):517–530
72. Harris JA (1998) Using c-fos as a neural marker of pain. Brain Res Bull 45(1):1–8
73. Hallbeck M, Larhammar D, Blomqvist A (2001) Neuropeptide expression in rat paraventricular hypothalamic neurons that project to the spinal cord. J Comp Neurol 433(2):222–238
74. Hallbeck M, Blomqvist A (1999) Spinal cord-projecting vasopressinergic neurons in the rat paraventricular hypothalamus. J Comp Neurol 411(2):201–211
75. Suryavanshi P et al (2022) Action Potentials Are Critical for the Propagation of Focally Elicited Spreading Depolarizations. J Neurosci 42(11):2371–2383
76. Eikermann-Haerter K, Can A, Ayata C (2012) Pharmacological targeting of spreading depression in migraine. Expert Rev Neurother 12(3):297–306
77. Ayata C, Lauritzen M (2015) Spreading Depression, Spreading Depolarizations, and the Cerebral Vasculature. Physiol Rev 95(3):953–993
78. Yousef Yengej D et al (2022) Different characteristics of cortical spreading depression in the sleep and wake states. Headache 62(5):577–587
79. Yousef Yengej DN et al (2021) Continuous long-term recording and triggering of brain neurovascular activity and behaviour in freely moving rodents. J Physiol 599(20):4545–4559
80. Li YJ et al (2023) Paraventricular nucleus-central amygdala oxytocinergic projection modulates pain-related anxiety-like behaviors in mice. CNS Neurosci Ther 29(11):3493–3506
81. Greco R et al (2013) Effect of sex and estrogens on neuronal activation in an animal model of migraine. Headache 53(2):288–296
82. Condes-Lara M et al (2009) Paraventricular hypothalamic oxytocinergic cells responding to noxious stimulation and projecting to the spinal dorsal horn represent a homeostatic analgesic mechanism. Eur J Neurosci 30(6):1056–1063

Publisher's Note